Inorganic Chemistry

Article

pubs.acs.org/IC

Magnetostructural *D* Correlations in Hexacoordinated Cobalt(II) Complexes

Ján Titiš* and Roman Boča

Department of Chemistry (FPV), University of SS. Cyril and Methodius, SK-917 01 Trnava, Slovakia

Supporting Information

ABSTRACT: The magnetostructural *D* correlation for hexacoordinated cobalt(II) complexes is outlined. The structural and magnetic properties of a series of mononuclear cobalt(II) complexes with the general formulas $[Co^{II}(L)_6]X_2$, $[Co^{II}(L)_2X_2]$, and $[Co^{II}(L)_2(H_2O)_2(car)_2]$ have been investigated where the coordination sphere is formed by nitrogen/oxygen-donor heterocycle (L), carboxylato (car), aqua, and chlorido ligands. The chromophores of these compounds involve $\{CoN_6\}$, $\{CoO_6\}$, $\{CoO_4O'_2\}$, $\{CoN_2O_2O'_2\}$, and $\{CoN_2O_2Cl_2\}$. All complexes were subjected to magnetochemical investigation down to 2 K (SQUID susceptibility and magnetization measurements). Most of the studied complexes show magnetic behavior typical for zero-field-splitting systems. The magnetism of the complex $[Co(H_2O)_6](6\text{-OHnic})_2$ reflects the presence of the magnetic angular momentum in the ground-state crystal-field term. The obtained values of the magnetic anisotropy (*D* or *δ*) have been correlated with the structural distortion of the coordination polyhedron. This correlation can be understood with the help of crystal-field theory, where the magnetic anisotropy parameters are related to the splitting of the lowest crystal-field multiplets.

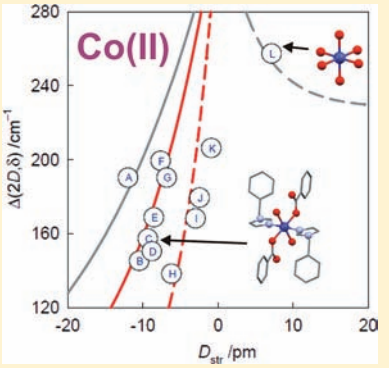

INTRODUCTION

Searching for well-defined relationships between different structural factors and the magnetic anisotropy in transition-metal complexes is very important for a rational design of new magnetic materials.[1] At this respect, particular attention deserves complex systems containing metal ions with unquenched orbital angular momentum ($L \neq 0$) because of their strong magnetic anisotropy.[2]

Magnetic as well as structural properties of the hexacoordinated cobalt(II) complexes are dominated by the fact that the ground-state electron term in the ideal octahedral geometry ($^4T_{1g}$) is orbitally degenerate. The first-order spin−orbit coupling mechanism splits this term into three groups of multiplets with $J = {}^1/_2$ (2×), ${}^3/_2$ (4×), and ${}^5/_2$ (6×), which can be efficiently handled using the Griffith approach.[3] In practice, however, it is impossible to meet an ideal octahedral configuration because the $^4T_{1g}$ term is subjected to the Jahn−Teller (JT) effect associated with geometry distortions. On tetragonal compression, the ground-state crystal-field term is $^4A_{2g}$ (Figure 1). It becomes well isolated from the excited-state ^4E_g term with increasing tetragonality $\Delta_{ax} = E(^4E_g) - E(^4A_{2g})$. This is a favorable situation because the second-order spin−orbit coupling splits the $^4A_{2g}$ manifold into a set of multiplets $E_{1/2}$ (2×) and $E_{3/2}$ (2×) which can be simply treated within the traditional spin-Hamiltonian (SH) formalism.[4] Therefore, the zero-field-splitting (ZFS) energy gap is $E(E_{3/2}) - E(E_{1/2}) = 2D$. A qualitatively different situation occurs on tetragonal elongation. In this case, the ground-state crystal-field term is ^4E_g, which carries first-order orbital magnetism. A suitable basis set to be considered is then spanned by the functions $|$

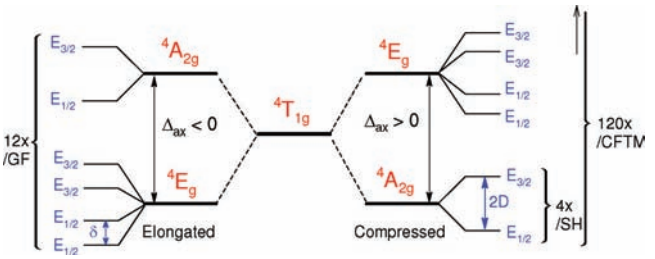

Figure 1. Scheme of the low-lying energy levels for the d^7 ion in near-octahedral configurations (not to scale). Griffith−Bethe notation: $E_{1/2} = \Gamma_6$, $E_{3/2} = \Gamma_7$.

$LSM_LM_S\rangle$; this ultimately demands an application of the extended Griffith−Figgis formalism.[3] It can be shown that the energy gap that is responsible for the anisotropic magnetic behavior now appears between the levels of the same symmetry $E(E_{1/2}) - E(E_{1/2}) = \delta$ (Figure 1). The above-described models utilize a limited basis set of the lowest-lying crystal-field terms and are mainly used for fitting the experimental data. The most complete theoretical insight provides a generalized crystal-field theory of multiplets (CFTM) working in the 120-membered basis set spanned by all electron terms arising from the d^7 electron configuration.[3] Within this approach, the magnetic properties can be efficiently modeled under the effect of principal electronic structure parameters (Racah repulsion parameters *B* and *C*, spin−orbit coupling constant *ξ*, and the

Received: September 28, 2011
Published: October 26, 2011

   dx.doi.org/10.1021/ic202108j | *Inorg. Chem.* 2011, 50, 11838–11845

Table 1. Structural Parameters for the Cobalt(II) Complexes Sorted According to D_{str}

no.[a]	donor set	d(Co−L) /Å[b]	D_{str}/pm [c]	E_{str}/pm	Σ/deg	ref (CCDC code or no.)
A	$N_2O_2O'_2$	O^w, 2.170; O, 2.122; N, 2.127	−11.90	2.42	1.08	17 (SENDUL)
B	$O_4O'_2$	O^w, 2.111; O, 2.109; O, 2.015	−9.40	0.10	2.82	18(KIJXIL02)
C	$N_2O_2O'_2$	O^w, 2.115; O, 2.140; N, 2.135	−9.25	1.25	2.22	19(831599)
D	$N_2O_2Cl_2$	O, 2.034; Cl, 2.492; N, 2.081	−8.70	3.40	2.24	20(796703)
E	$N_2O_2O'_2$	O^w, 2.140; O, 2.069; N, 2.120	−8.45	3.55	5.57	21(APICCO04)
F	$N_2O_2O'_2$	O^w, 2.124; O, 2.079; N, 2.126	−7.55	2.35	1.97	22(PIBFOW01)
G	$N_2O_2O'_2$	O^w, 2.140; O, 2.083; N, 2.144	−6.75	2.85	1.96	23(POFXOY)
H	N_6	N, 2.143; N, 2.197; N, 2.211	−6.10	0.71	2.37	24(NERBES)
I	$N_2O_2O'_2$	O^w, 2.121; O, 2.085; N, 2.175	−2.80	1.80	0.91	19(831600)
J	$N_2O_2O'_2$	O^w, 2.109; O, 2.079; N, 2.171	−2.30	1.50	0.73	19(831601)
K	$N_2O_2O'_2$	O^w, 2.107; O, 2.085; N, 2.188	−0.80	1.10	1.53	19(831602)
L	O_6	O^w, 2.113; O^w, 2.042	+7.23	0	1.87	25(AJIDON)

[a] **A** $[Co(MeIz)_2(ac)_2(H_2O)_2]$, **B** $[Co(2\text{-}OHnic)_2(H_2O)_2]$, **C** $[Co(bylim)_2(bz)_2(H_2O)_2]$, **D** $[CoL_2Cl_2]\cdot 3.5H_2O$, **E** $[Co(pic)_2(H_2O)_2]\cdot 2H_2O$, **F** $[Co(2\text{-}MeSnic)_2(Me_2fpy)_2(H_2O)_2]$, **G** $[Co(bz)_2(nca)_2(H_2O)_2]$, **H** $[Co(Iz)_6](fm)_2$, **I** $[Co(iqu)_2(ac)_2(H_2O)_2]$, **J** $[Co(1\text{-}py\text{-}bzfpy)_2(ac)_2(H_2O)_2]$, **K** $[Co(bzfpy)_2(ac)_2(H_2O)_2]$, **L** $[Co(H_2O)_6](6\text{-}OHnic)_2$. Abbreviations for ligands: Iz = 1*H*-imidazole, fm = formiate, 2-OHnic = 2-hydroxynicotinate, 6-OHnic = 6-hydroxynicotinate, bzfpy = benzofuro[3,2-*c*]pyridine, bylim = 1-phenyl-1*H*-imidazole, bz = benzoate, pic = picolinate, iqu = isoquinoline, MeIz = 1-methylimidazole, ac = acetate, 2-MeSnic = 2-methylthionicotinate, Me_2fpy = 2,3-dimethylfuro[3,2-*c*]pyridine, 1-py-bzfpy = 1-(pyridin-3-yl)benzofuro[3,2-*c*]pyridine, nca = nicotinamide, L = 2-[(2,2-diphenylethylimino)methyl] pyridine-1-oxide). [b] w = aqua ligand. [c] $D_{str} < 0$, compressed bipyramid; $D_{str} > 0$, elongated bipyramid.

crystal-field strengths F_4 and F_2), which provides useful predictions.

Well-known systematic studies of the magnetic coupling as a function of the geometric elements and chemical identity of the bridging ligands in dinuclear complexes proved to be very useful for molecular magnetism.[5] Recently, a new type of such magnetostructural correlation has been reported for a series of mononuclear nickel(II) complexes, where the axial ZFS parameter D has been correlated with the tetragonal distortion D_{str}.[6,7] In the case of hexacoordinated nickel(II) complexes, the D values are negative for a compressed tetragonal bipyramid, approaching 10 cm^{-1}. For the Co^{II} ion, the D is much larger (10^2 cm^{-1}) and positive. However, in polynuclear systems, an overall Ising-type anisotropy ($D_{mol} < 0$) can be obtained by the appropriate orientation of the local ZFS tensors with respect to the molecular easy axis.[8]

In this work, the experimental and theoretical magneto-structural studies on the series of mononuclear high-spin cobalt(II) complexes have been carried out and attempts have been made to correlate the single-ion magnetic anisotropy with the relevant structural parameters. The series is represented by $\{CoN_6\}$, $\{CoO_6\}$, $\{CoO_4O'_2\}$, $\{CoN_2O_2O'_2\}$, and $\{CoN_2O_2Cl_2\}$ types of chromophores.

EXPERIMENTAL SECTION

Synthesis. Syntheses and detailed characterization (elemental analyses and NMR, IR, and electronic spectroscopy) of the studied complexes and some ligands have been already published separately (see the references in Table 1).

Physical Measurements. Single-crystal X-ray diffraction experiments have been performed using a Gemini R CCD apparatus (Oxford Diffraction). Data reduction and analytical absorption corrections were performed with the *CrysAlisPro* package.[9,10] The structures were solved by direct methods using *SIR-97* or *SHELXS-97* and refined by the full-matrix least-squares procedure with *SHELXL-97*.[11,12] Geometrical analyses were performed with the *MERCURY* program. The structural data of all complexes have been deposited in the Cambridge Crystallographic Data Centre.[13]

Magnetic susceptibility and magnetization measurements were done using a SQUID magnetometer (Quantum Design, MPMS-XL7) between 2 and 300 K at B = 0.1 T. The magnetization data until B = 6 and/or 7 T were taken at T = 2.0 and 4.6 K, respectively. Raw susceptibility data were corrected for underlying diamagnetism using the set of Pascal constants. The effective magnetic moment has been calculated as usual: $\mu_{eff}/\mu_B = 798(\chi' T)^{1/2}$ when SI units are employed.

RESULTS AND DISCUSSION

Structural Data. Except the distortions activated by the JT effect (owing to the orbitally degenerate $^4T_{1g}$ ground-state term in an octahedral configuration), some other factors are operative on the actual geometry of the coordination polyhedron of d^7 systems (such as binding anisotropy within the chromophore or solid-state effects). As a measure of departure from the perfect octahedral symmetry, we proposed the following set of structural parameters: the axial asymmetry parameter D_{str}, the rhombic asymmetry parameter E_{str}, and the Σ parameter specifying the angular deformations.

The radial structural parameters (D_{str} and E_{str}) were originally defined for homoleptic complexes;[14] in the case of a heterogeneous donor set, they are corrected as follows:[15]

$$D_{str} = (d_i - \bar{d}_i)_z - [(d_i - \bar{d}_i)_x + (d_i - \bar{d}_i)_y]/2 \quad (1)$$

$$E_{str} = [(d_i - \bar{d}_i)_x - (d_i - \bar{d}_i)_y]/2 \quad (2)$$

where $\bar{d}_i$ is the mean distance for a given bond (in this case i = N, O, Cl). Values of $\bar{d}_i$ have been taken from compounds containing the $[Co(NH_3)_6]^{2+}$, $[Co(H_2O)_6]^{2+}$, and $[CoCl_6]^{4-}$ complex units, giving rise to $\bar{d}$(Co−N) = 2.185 Å, $\bar{d}$(Co−O) = 2.085 Å, and $\bar{d}$(Co−Cl) =2.475 Å (Figure 2).[16]

Equations 1 and 2 satisfy the conditions $E_{str} > 0$ and $|E_{str}/D_{str}| \leq {}^1/_3$; those are usual in electron spin resonance (ESR) and magnetochemistry. The angular distortion parameter Σ is derived from 12 L−M−L bond angles φ_i as follows:

$$\Sigma = \left(\sum_i |\phi_i - 90|\right)/12 \quad (3)$$

It is equal to zero for an ideal octahedron and increases with its distortions.

A total of 12 structurally well-characterized cobalt(II) compounds are involved in this study (Figure 3). Their coordination sphere in the first approximation can be viewed as distorted octahedral. Taking the above definitions, the effective

dx.doi.org/10.1021/ic202108j | *Inorg. Chem.* 2011, 50, 11838–11845

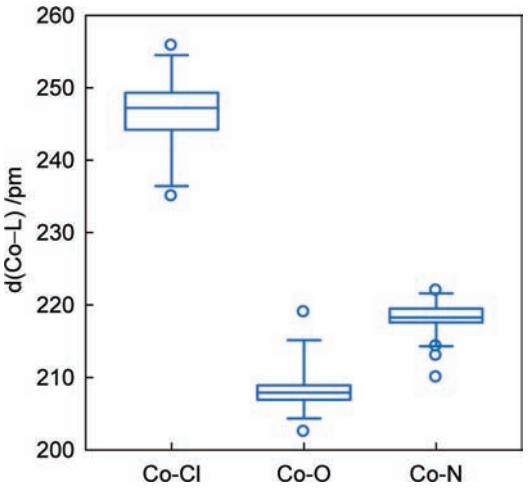

Figure 2. Statistics of the Co–L bonds for a series of $[CoCl_6]^{-4}$, $[Co(H_2O)_6]^{2+}$, and $[Co(NH_3)_6]^{2+}$ reference complexes. The line in the box indicates the median value of the data, which has been assigned as $\bar{d}_i$.

distortion for these complexes has been refined to a compressed and elongated tetragonal, respectively, with smaller or larger rhombic contribution. The selected bond distances and calculated distortion parameters are listed in Table 1. Detailed information about the crystallographic results can be found in the appropriate literature.

Three complexes possess a homogeneous donor set: $\{CoN_6\}$, $\{CoO_4O'_2\}$, and $\{CoO_6\}$. In the complex **H**, the cobalt atom is situated in an environment of six tertiary nitrogen atoms of the imidazole ligands. The bond distances involved in this geometry yield $D_{str} = -6.10$ pm, which refers to a compressed tetragonal bipyramid. More detailed insight into the structure of the compound shows that the imidazole units are strongly involved in the 3D network of hydrogen bonds via formiate anions. The nickel(II) analogue of the complex **H** shows $D_{str} = +3.50$ pm, which refers to an elongated bipyramid.[14]

In complex **B**, the central Co^{II} ion is located in the center of symmetry, and it is coordinated by six oxygen atoms, forming a nearly regular compressed tetragonal bipyramid. The basal plane of the bipyramid is formed by the oxygen atoms of the hydroxyl group of 2-hydroxynicotinato and the oxygen atoms of the aqua ligands. The axial sites are occupied by one of the carboxylato oxygen atoms at a much shorter Co–O distance. Compound **L** contains the hexaaquacobalt(II) cations, forming an elongated bipyramid ($D_{str} = +7.23$ pm); two 2-hydroxynicotinate anions are the counterions. These units are involved in an extensive system of hydrogen bonds.

Eight complexes, **A**, **C**, **E**–**G**, **I**, **J**, and **K**, possess a centrosymmetric arrangement of ligands with orthorhombic $\{CoN_2O_2O'_2\}$ chromophores. In these cases, the axial positions are formally occupied by nitrogen-donor heterocyclic ligands, while the equatorial plane is formed by aqua ligands and

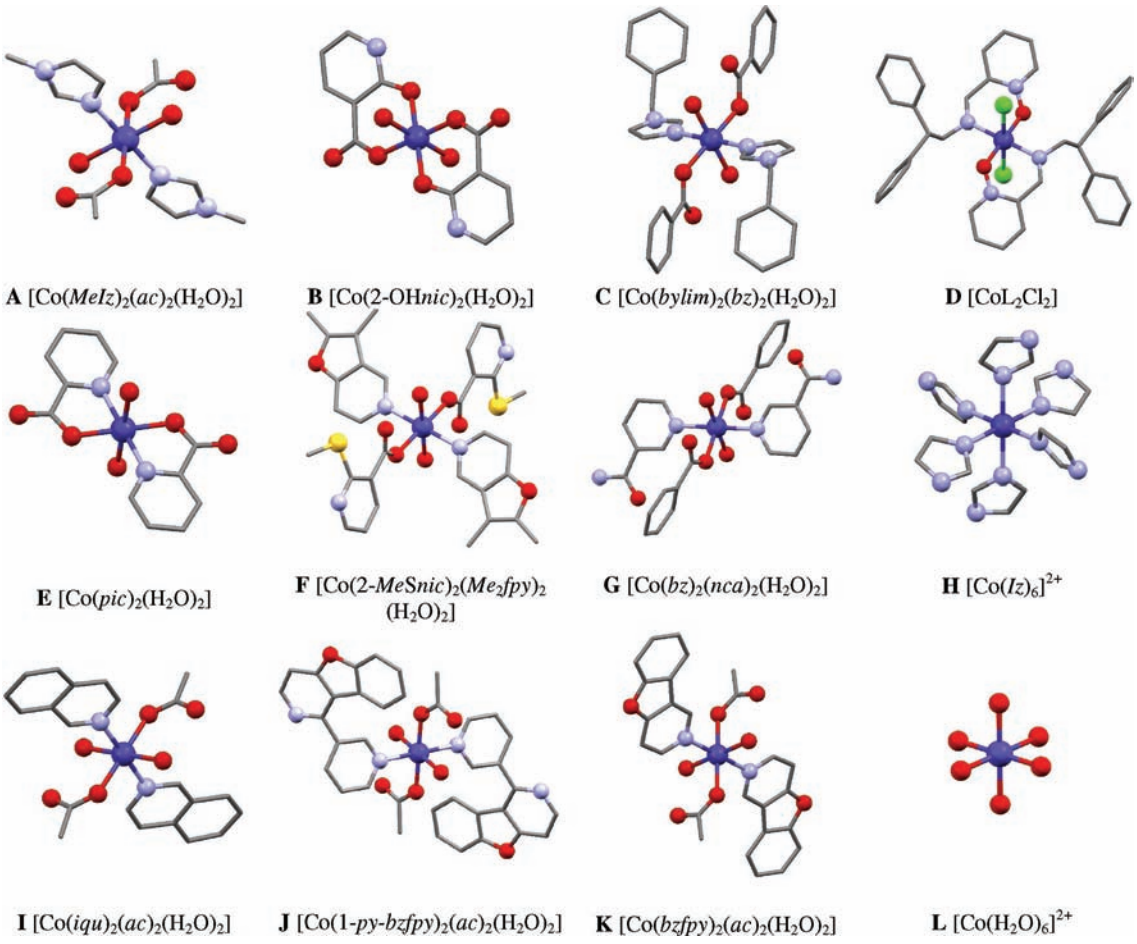

Figure 3. Molecular structures of the complexes studied (hydrogen atoms are omitted for clarity).

dx.doi.org/10.1021/ic202108j | Inorg. Chem. 2011, 50, 11838–11845

carboxylato anions bonded in a unidentate manner. However, just because of the presence of the heterogeneous donor set, determination of the effective distortion is slightly complicated for such complexes. Note that for complexes **I**–**K** the condition for E/D is not met and thus choice of the correct axes (e.g., $|Co-N|_{ax}$, $|Co-O^{w}|_{eq}$, and $|Co-O|_{eq}$) is questionable. In order to bring some light to this problem, we analyzed the relationship between the crystal-field parameter $F_4(R)$ and the lengths of the Co–N, Co–O, and Co–Cl bonds, respectively. The procedure is essentially described by the following stages: (i) we start from the simple definition $F_4(R) = A_4(R)R^{-5}$; for a given bond type, the factor $A_4(R)$ has been estimated using the $\bar{d}_i$ and $10Dq = f_L g_M$ of $[CoCl_6]^{4-}$, $[Co(H_2O)_6]^{2+}$, and $[Co(NH_3)_6]^{2+}$ (see the Supporting Information); (ii) for the studied complexes, the estimated $A_4(R)$ and crystallographic d_i values have been used to evaluate $F_4(R)$ of the considered bond. A graphical representation of the analysis is shown in Figure 4. We can conclude the following:

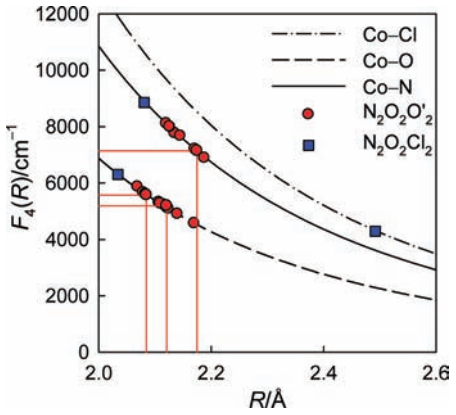

Figure 4. Crystal-field analysis of the metal–ligand interaction in complexes with a heterogeneous donor set. Drop lines belong to complex **J**.

for all $\{CoN_2O_2O'_2\}$ complexes, nitrogen-donor ligands generate a stronger crystal field than a pair of oxygen donors; $F_4(Co-N) > \{F_4(Co-O^{w}), F_4(Co-O)\}$. This means that the choice of $|Co-N|_{ax}$, $|Co-O^{w}|_{eq}$, and $|Co-O|_{eq}$ is probably correct, and the effective distortions refer to a compressed tetragonal bipyramid. In this series of compounds, complex **A** possesses the largest tetragonality (D_{str} = −11.90 pm).

Complex **D** contains the $\{CoN_2O_2Cl_2\}$ chromophore. Here, the chlorido ligands occupy formal positions of the aqua ligands and the carboxylato oxygen donors are replaced by neutral nitrogen oxides. This complex structurally falls to the region that is typical for axially compressed cobalt(II) structures (D_{str} = −8.70 pm). Its rhombicity is relatively large (E_{str} = +3.40 pm). Throughout the series, complex **E** displays the largest deviation from an ideal axial symmetry. In particular, there is a significant contribution from angular deformations (Σ = 5.57°).

The above discussion shows that structural distortion of the cobalt(II) complexes appears as a consequence of interplay between local vibronic and crystal environment effects. In order to determine the dominant driving force of such structural changes, Atanasov et al. carried out a density functional theory study for hexacyanometalates $[M(CN)_6]^{n-}$ with T_g ground-state terms.[26] It has been concluded that the JT distortion is very weak for Ti^{III}, V^{III}, and Fe^{III} (ca. 1 pm) and larger for Mn^{III}, Mn^{II}, and Cr^{II} (of about 4 pm). In the aforementioned work, the metal–ligand π-bonding effects have been considered as a main factor that determines the final sign and magnitude of the JT distortion. On the basis of these results, we can assume that solid-state effects represent the dominant contribution to the overall structural distortion even in the case of the T_g ground-state systems.

Magnetic Data. The temperature and field dependence of magnetization have been measured for all complexes using a SQUID apparatus. Temperature-dependent data were transformed to the molar susceptibility and subsequently to the effective magnetic moment. Figure 5 compares the SQUID data of two exemplary structures: **B** (compressed bipyramid) and **L** (elongated bipyramid). A complete set of the magnetic data for cobalt(II) complexes under study are shown in Figure S1 in the Supporting Information.

Magnetic data of complexes with negative D_{str} are consistent with the ZFS. On cooling, the effective magnetic moment stays almost constant at its room temperature $\mu_{eff} \approx 5.0\ \mu_B$ until 150–100 K, when it gradually decreases to a value of $\mu_{eff} \approx 3.5–4.0\ \mu_B$ at T = 2 K. Magnetization at T = 2.0 K saturates to the value of $M_{mol}/N_A\mu_B \approx 2.0–2.4$.

The low-temperature susceptibility data are dominated by the lower Kramers doublet $M_S = \pm^1/_2$, and the limiting value is $\mu_{eff}(LT) = (g_z^2/4 + 2g_x^2)^{1/2}\mu_B$ irrespective of D. With g_z = 2.0

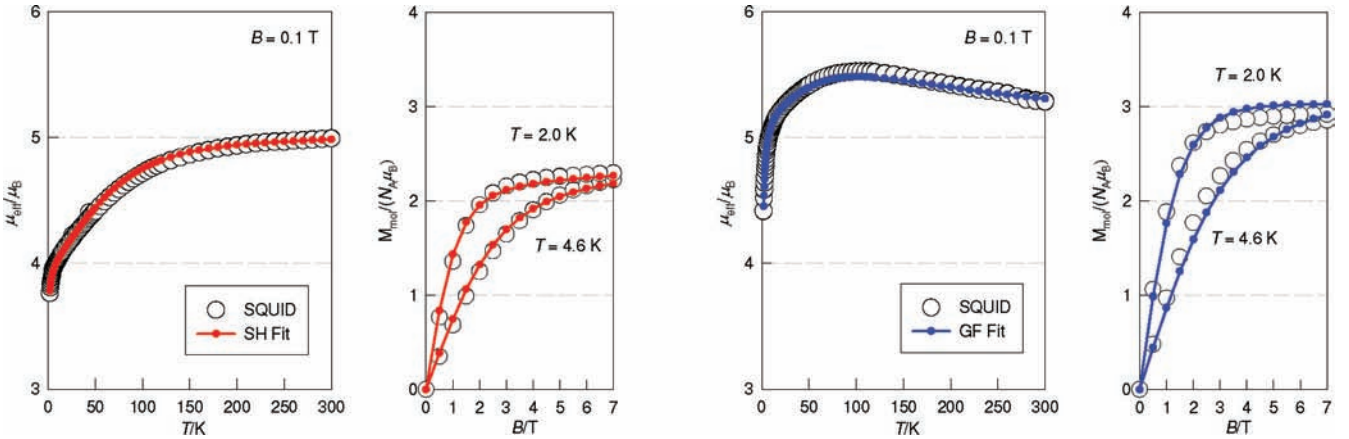

Figure 5. Comparison of magnetic data for complexes **B** (left) and **L** (right). Typical patterns of the temperature dependence of the effective magnetic moment for tetragonally compressed and elongated cobalt(II) structures are shown.

dx.doi.org/10.1021/ic202108j | Inorg. Chem. 2011, 50, 11838–11845

and typical $g_x = 2.7$, one gets $\mu_{eff}(LT) = 3.95\ \mu_B$. Lower values observed at $T \sim 2$ K are attributed to the presence of intermolecular interactions described by the molecular-field correction. The high-temperature limit is $\mu_{eff}(HT) = [(g_z^2 + 2g_x^2)(5/4)]^{1/2}\mu_B$, which with the above typical values yields 4.23 μ_B again irrespective of D.

Magnetic parameters were determined using a fitting procedure in which the energy levels result from a full-matrix diagonalization of the SH:

$$\hat{H}^S = \hbar^{-2}[D(\hat{S}_z^2 - \hat{S}^2/3) + E(\hat{S}_x^2 - \hat{S}_y^2)] + \hbar^{-1}\mu_B(\vec{B}\cdot\bar{\bar{g}}\cdot\vec{S}) \quad (4)$$

We note the following: (i) SH modeling of spin levels shows that the E parameter modifies the ZFS gap but causes no additional splitting of the Kramers doublets (Figure S2 in the Supporting Information). Determination of E is, therefore, possible only at saturation fields of magnetization where the spin levels are split enough (Figure S3 in the Supporting Information). (ii) In the previous work, we showed that the minor molecular-field correction is essential in reproducing the low-temperature susceptibility data for $T < 10$ K;[27] thus, the calculation has been improved by the correction

$$\chi_{cor} = \chi/[1 - (zj/N_A\mu_0\mu_B^2)\chi] + \alpha \quad (5)$$

where the parameter zj includes the isotropic exchange interaction j with the number of nearest neighbors z; the parameter α compensates for uncertainties in determining the underlying diamagnetism, and it accounts for the temperature-independent paramagnetism; χ is the net molar magnetic susceptibility. The susceptibility dataset (χ vs T at $B = 0.1$ T) as well as the magnetization dataset (M vs B at $T = 2.0$ and 4.6 K) has been treated simultaneously. They were used in the construction of a common functional to be optimized by the same set of magnetic parameters: g_x, g_y, D, E, zj, and α. The z component of the g factor (g_z) has been fixed to 2.0 (as predicted by crystal-field theory).[3] The optimum set of magnetic parameters is listed in Table 2.

Table 2. SH Parameters for Complexes with Negative D_{str}

no.	g_x	g_y	D/cm^{-1}	E/cm^{-1}	zj/cm^{-1}	α^a	R/%
A	2.53	2.53	95.00	0	−0.08	+16.72	0.43
B	2.67	2.73	73.91	0.26	−0.02	+5.43	0.81
C	2.51	2.62	79.99	0.55	−0.05	+18.22	0.99
D	2.35	2.51	73.10	4.81	−0.01	−9.01	0.67
E	2.65	2.72	84.24	2.34	−0.05	+6.01	1.29
F	2.74	2.61	99.54	1.39	−0.01	+4.36	0.96
G	2.972	3.124	94.34	1.47	0	0	1.81
H	2.753	2.753	69.21	0	−0.01	0	0.48
I	2.587	2.689	85.96	3.01	−0.01	+2.04	0.49
J	2.607	2.758	87.59	2.84	−0.01	−6.49	0.83
K	2.613	2.801	103.10	6.90	−0.14	+0.23	0.54

^{a}In 10^{-9} m^3 mol^{-1}.

The susceptibility data (μ_{eff} vs T) of complexes with positive D_{str} are characterized by a typical pattern showing a broad maximum that is clearly visible for complex **L**. In this case, the Figgis anisotropic Hamiltonian for the $^4T_{1g}$ parent term on symmetry lowering is appropriate. Modeling of the temperature dependence of the effective magnetic moment within this theory confirms the existence of the maximum, but that, as can be seen in Figure S4 in the Supporting Information, can be shifted far over 300 K. For analysis of the experimental data, the following form of the Figgis Hamiltonian has been applied:[28,29]

$$\hat{H} = \Delta_{ax}[\hbar^{-2}\hat{L}_z^2 - L(L+1)/3] - \hbar^{-2}J_{12}(\vec{L}\cdot\vec{S}) + \hbar^{-1}\mu_B\vec{B}\cdot(g_L\vec{L} + g\vec{S}) \quad (6)$$

The independent magnetic parameters that should be fixed by the fitting procedure are $g_L = -A\kappa$ (A, Figgis CI parameter; κ, orbital reduction factor; ranging between $-1.5 \le g_L \le -\kappa$) and the crystal-field splitting Δ_{ax}; the isotropic g factor is assumed ($g = 2$). The coupling parameter is constrained through the relationship $J_{12} = -(\xi/2S)A\kappa$ with the spin−orbit coupling constant $\xi = 515$ cm^{-1}. The resulting set of parameters is $\Delta_{ax} = -112$ cm^{-1}, $J_{12} = -188$ cm^{-1}, and $g_L = -1.10$. These parameters were used to reconstruct the appropriate multiplets using the zero-field secular equations for the $^4T_{1g}$ term under symmetry lowering.[3] The equations factored to blocks along with the calculated energies are presented in Table 3.

Correlation of Data. On passing from the octahedral geometry to the tetragonal bipyramid, the axial structural anisotropy can be characterized by the asymmetry parameter D_{str}, while the magnetic anisotropy is conventionally described by the axial ZFS parameter D. It can therefore be expected that there will be some interrelation between these parameters. An approximately linear correlation has been found for nickel(II) complexes, where with the increasing axial distortion (from compression to elongation) the magnetic anisotropy D also increases. This relationship has been termed the magneto-structural D correlation.[7] However, such a simple relationship cannot be expected for the cobalt(II) complexes whereupon tetragonal distortion (from minus to plus) the ground-state electronic state changes from $^4A_{2g}$ (compressed bipyramid) to $^4T_{1g}$ (octahedron) and ^4E_g (elongated bipyramid), respectively.

First, we will investigate the ZFS resulting from the set of crystal-field parameters [B, C, $F_4(z)$, $F_4(xy)$, and ξ] that offers insight into the origin of the ZFS and help in the analysis of the experimental data. For such a target, we adopted crystal-field theory in the generalized form (allowing an arbitrary position of the ligands) with the aim of calculating the energy levels: crystal-field terms → crystal-field multiplets. ZFS is then defined in the context of Figure 1 as $\Delta = 2D = E(E_{3/2}) - E(E_{1/2}) > 0$ and $\Delta = \delta = E(E_{1/2}) - E(E_{1/2}) > 0$, respectively. In this calculation, all of the matrix elements of the relevant operators were evaluated in the basis set of free-atom terms using the irreducible tensor operators approach.[3] In the previous paper, we presented the result as a 3D model, i.e., $\Delta(2D,\delta) = f\{F_4(z),F_4(xy)\}$, where F_4 are crystal-field multipoles in axial and equatorial positions, respectively (Figure S5 in the Supporting Information).[27] Here we apply a transform of $F_4(z)$ and $F_4(xy)$ into a single D_{str} parameter in order to obtain a single-parameter function $\Delta = f(D_{str})$.

In crystal-field theory, the pole strength $F_4(R)$ varies with the bond length as $A_4(R)R^{-5}$, where the factor A_4 depends on the charge of the ligand and the mean distance of the d electrons from the nucleus. Thus, the definition of the axial asymmetry parameter ($D_{str} = R_{ax} - R_{eq}$) and assumption that A_4 remains common for the axial and equatorial ligands lead to the equation

dx.doi.org/10.1021/ic202108j | Inorg. Chem. 2011, 50, 11838–11845

Table 3. Secular Equations for $^4T_{1g}$ and Calculated Multiplet Energies for L

Factored interaction matrix [a]	IRs	$E(\Gamma)$ [b]	$E(\Gamma)$ shifted [b]
$\lambda\begin{pmatrix} \nu/3+3g_L/2 & \sqrt{3/2}g_L & 0 \\ \sqrt{3/2}g_L & -2\nu/3 & \sqrt{2}g_L \\ 0 & \sqrt{2}g_L & \nu/3+3g_L/2 \end{pmatrix}\rightarrow$	$\Gamma_6(E_{1/2})$	−477	0 (ground state)
	$\Gamma_6(E_{1/2})$	−219	257 (δ)
	$\Gamma_7(E_{3/2})$	317	794
$\lambda\begin{pmatrix} \nu/3-g_L/2 & \sqrt{3/2}g_L \\ \sqrt{3/2}g_L & -2\nu/3 \end{pmatrix}\rightarrow$	$\Gamma_7(E_{3/2})$	−165	311
	$\Gamma_6(E_{1/2})$	297	774
$\lambda(\nu/3-3g_L/2)\rightarrow$	$\Gamma_7(E_{3/2})$	246	723

[a] $\nu = \Delta_{ax}/\lambda$. [b] In cm^{-1}.

$$D_{str} = R_{ax} - R_{eq} \approx R_{ax}\{1 - [F_4(z)/F_4(x)]^{1/5}\} = R_{ax}\cdot X_F \quad (7)$$

which transforms the F_4 poles to the structural ordinate.[6] Calculations for different octahedral and tetragonal configurations are shown in Figure 6a. From this figure, we can see the following: (i) ZFS energy gaps, and thus the magnetic anisotropy, strongly decrease with the axial distortions; (ii) for the octahedron, the energy gap reaches the maximum value of ~350 cm^{-1}; (iii) minimum values are ~50 cm^{-1} for the compressed bipyramid and ~210 cm^{-1} for the elongated bipyramid.

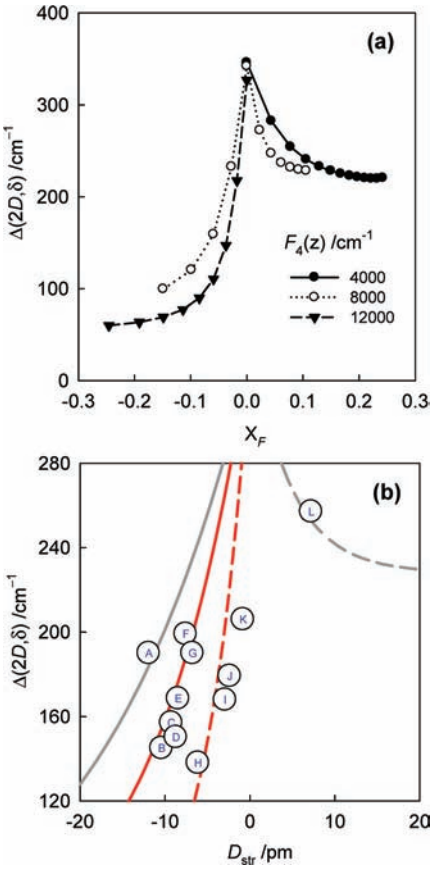

Figure 6. Magnetostructural D correlation for the cobalt(II) complexes. (a) CFTM modeling of the magnetic anisotropy for the tetragonally compressed and elongated systems: $F_4(xy)$ = 4000−12 000 cm^{-1}, B = 789 cm^{-1}, C/B = 4.3, and ξ = 515 cm^{-1}. (b) Correlation of the experimental data: circles. Correlation curves: lines.

The experimental ZFS values for the set of cobalt(II) complexes plotted as a function of the structural D_{str} parameter (Figure 6b) exhibit behavior similar to that obtained from the CFTM calculations. Tetragonally compressed structures span the interval of $2D \approx 150-205$ cm^{-1}. This dataset splits into three subsets ({**A**}, {**B**−**G**}, and {**H**−**K**}), two of which have been fitted on a three-parameter exponential function. The results are as follows:

for **B**−**G** (R^2 = 0.757)

$$2D = 38 + 296\exp(0.09D_{str}) \quad \text{with } D\ (cm^{-1}) \text{ and } D_{str}\ (pm) \quad (8)$$

for **H**−**K** (R^2 = 0.384)

$$2D = 42 + 288\exp(0.20D_{str}) \quad \text{with } D\ (cm^{-1}) \text{ and } D_{str}\ (pm) \quad (9)$$

The correlation for **A** can only be estimated, and it is

$$2D = 28 + 300\exp(0.05D_{str}) \quad \text{with } D\ (cm^{-1}) \text{ and } D_{str}\ (pm) \quad (10)$$

The tetragonally elongated complex **L** adopts a markedly larger δ value, 257 cm^{-1}. For this complex, the estimated correlation is

$$\delta = 228 + 114\exp(-0.21D_{str}) \quad \text{with } \delta\ (cm^{-1}) \text{ and } D_{str}\ (pm) \quad (11)$$

From the structural data of the studied complexes, an importance of the nonaxial deformations (radial in-plane distortions as well as different angular distortions) can be extracted, which, of course, also contributes to the ZFS. We investigated such contributions using CFTM theory, namely, $D_{4h} \rightarrow D_{2h}$ (radial), $D_{4h} \rightarrow D_{2d}$ (angular), and $D_{4h} \rightarrow C_{2v}$ (angular) (Figure 7). For the first (rhombic) distortion, the transformation equation is

$$E_{str} = \frac{1}{2}(d_x - d_y) \approx d_x\frac{1}{2}\{1 - [F_4(x)/F_4(y)]^{1/5}\} = d_x\Xi_F \quad (12)$$

The $2D$ and δ values are then plotted against the Ξ_F function, which quantifies the lengthening and/or shortening of the M−L bond in the x direction. Two additional calculations represent

dx.doi.org/10.1021/ic202108j | Inorg. Chem. 2011, 50, 11838–11845

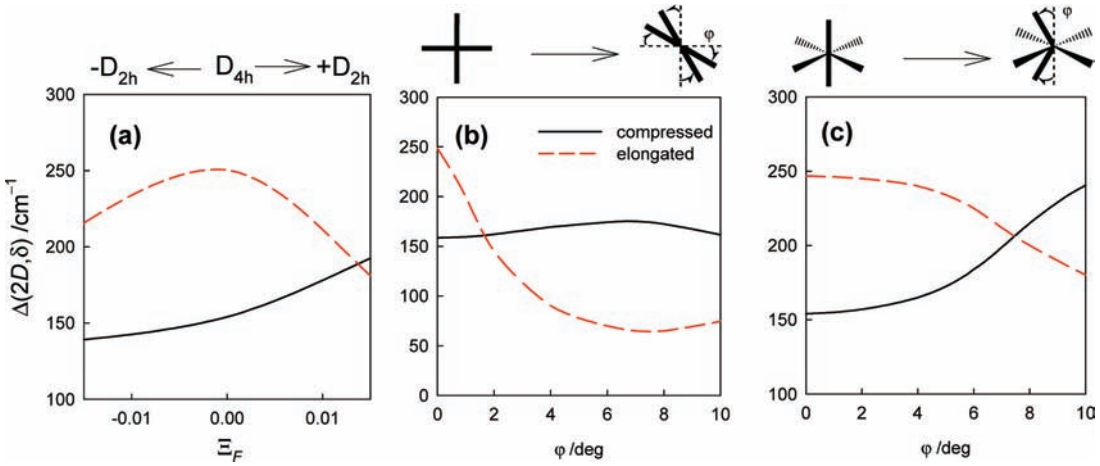

Figure 7. Evolution of the calculated ZFS values for the Co^{II} ion along (a) in-plane $D_{4h} \rightarrow D_{2h}$ (radial), (b) in-plane $D_{4h} \rightarrow D_{2d}$ (angular), and (c) axial $D_{4h} \rightarrow C_{2v}$ (angular) distortion paths.

a modeling of the in-plane (symmetric scissor squeeze) and axial (symmetric flexion) angular distortions, respectively. From Figure 7, one can withdraw the following findings: (a) for the elongated bipyramid, the asymmetry factor Ξ_F significantly decreases the ZFS in both directions; in the case of the compressed bipyramid, the ZFS increases in one direction and only slightly decreases in the other one; (b) for the elongated bipyramid, the ZFS rapidly decreases until 4°, while an increase for the compressed bipyramid is moderate; (c) C_{2v} distortion contributes to the ZFS slightly until 4° and then the course is much steeper.

It needs to be critically said that in the present case very high D values are reported and, consequently, the susceptibility data are a little sensitive to the energy gap $\Delta = 2D \sim 200\ cm^{-1}$. On the contrary, the magnetization data reflect the D values sensitively. Those values of D cannot be detected by ESR even with THz sources. However, far-IR spectroscopy facilitates the detection of such big values even in zero magnetic field. A total of 15 allowed transitions among the crystal-field multiplets that show the largest intensity increase on cooling refer to the energy gap $\Delta = 2D$.[27,30]

CONCLUSIONS

The ZFS of 12 hexacoordinated mononuclear cobalt(II) complexes has been analyzed by means of magnetostructural correlations. Structural as well as SQUID susceptibility and magnetization measurements confirm the effectively negative axial distortion (tetragonal compression) for 11 complexes, **A**–**K**. Positive distortion (tetragonal elongation) has been clearly confirmed only for complex **L**. Correlation of the structural and magnetic D parameters (in approximate D_{4h} symmetry) reveals the strongly decreasing relationship that can be appropriately described using the simple three-parameter exponential function.

In this study, we consider the ZFS in the form $\Delta = 2D$ for all complexes (D_{4h} approximation). However, the rhombicity of complexes with heterogeneous donor sets can be significant, and thus the rigorous form of the ZFS energy gap for such systems is $\Delta = 2(D^2 + 3E^2)^{1/2}$. We have studied theoretically the rhombic contributions to the ZFS along with some further nonaxial distortions. The key message is that in some specific cases the ZFS can be very sensitive to radial and angular low-symmetry deformations, particularly in elongated tetragonal configurations. Given that the low-symmetry effects are not included in our correlation, a more reliable outcome with less dispersion of the experimental data probably cannot be expected.

ASSOCIATED CONTENT

Supporting Information

Complete set of the fitted magnetic data and modeling of spin energy levels and magnetic functions. This material is available free of charge via the Internet at http://pubs.acs.org.

AUTHOR INFORMATION

Corresponding Author

*E-mail: jan.titis@ucm.sk. Tel.: +421 33 5921 408. Fax: +421 33 5921 403.

ACKNOWLEDGMENTS

Slovak Grant Agencies (VEGA 1/1005/09, 1/0052/11, and APVV-VVCE-0004-07) are acknowledged for financial support.

REFERENCES

(1) Gatteschi, D.; Sessoli, R.; Villain, J. *Molecular Nanomagnets*; Oxford University Press: Oxford, U.K., 2006.
(2) Lloret, F.; Julve, M.; Cano, J.; Ruiz-García, R.; Pardo, E. *Inorg. Chim. Acta* **2008**, *361*, 3432.
(3) Boča, R. *Struct. Bonding (Berlin)* **2006**, *117*, 1.
(4) Boča, R. *Coord. Chem. Rev.* **2004**, *248*, 757.
(5) Gorun, S. M.; Lippard, S. J. *Inorg. Chem.* **1991**, *30*, 1625.
(6) Boča, R.; Titiš, J. Magnetostructural *D*-correlations for Zero-Field Splitting in Nickel(II) Complexes. In *Coordination Chemistry Research Progress*; Nova: New York, 2008; p 247.
(7) Titiš, J.; Boča, R. *Inorg. Chem.* **2010**, *49*, 3971.
(8) Murrie, M. *Chem. Soc. Rev.* **2010**, *39*, 1986.
(9) Clark, R. C.; Reid J. S. *Acta Crystallogr., Sect. A* **1995**, *51*, 887.
(10) *CrysAlisPro*; Oxford Diffraction Ltd.: Abingdon, England, 2009.
(11) Altomare, A.; Burla, M. C.; Camalli, M.; Cascarano, G. L.; Giacovazzo, C.; Guagliardi, A.; Moliterni, A. G. G.; Polidori, G.; Spagna, R. *J. Appl. Crystallogr.* **1999**, *32*, 115.
(12) Sheldrick, G. M. *Acta Crystallogr.* **2008**, *A64*, 112.
(13) Cambridge Crystallographic Data Centre, http://www.ccdc.cam.ac.uk.
(14) Mašlejová, A.; Ivaniková, R.; Svoboda, I.; Papánková, B.; Dlháň, L.; Mikloš, D.; Fuess, H.; Boča, R. *Polyhedron* **2006**, *25*, 1823.

(15) Titiš, J.; Boča, R.; Dlháň, L.; Ďurčeková, T.; Fuess, H.; Ivaniková, R.; Mrázová, V.; Papánková, B.; Svoboda, I. *Polyhedron* **2007**, *26*, 1523.
(16) Inorganic Crystal Structure Database, Fachinformationszentrum Karlsruhe, Germany, http://www.fiz-informationsdienste.de/en/DB/icsd/index.html.
(17) Papánková, B.; Svoboda, I.; Fuess, H. *Acta Crystallogr.* **2006**, *E62*, m1916.
(18) Miklovič, J.; Segla, P.; Mikloš, D.; Titiš, J.; Herchel, R.; Melník, M. *Chem. Pap.* **2008**, *62*, 464.
(19) Titiš, J.; Hudák, J.; Kožíšek, J.; Krutošíková, A.; Moncol, J.; Tarabová, D.; Boča, R. *Polyhedron* **2011**, submitted.
(20) Rajnák, C.; Titiš, J.; Boča, R.; Moncol, J.; Padělková, Z. *Monatsh. Chem.* **2011**, *142*, 789.
(21) Papanková, B.; Boča, R.; Chnapková, V.; Dlháň, L.; Svoboda, I. Progress in Coordination and Bioinorganic Chemistry. *Proceedings of 19th International Conference on Coordination and Bioinorganic Chemistry*; STU Press: Bratislava Smolenice, Slovakia, June 2−6, 2003; p 279.
(22) Segla, P.; Miklovič, J.; Mikloš, D.; Titiš, J.; Herchel, R.; Moncol, J.; Kaliňáková, B.; Hudecová, D.; Mrázová, V.; Lis, T.; Melník, M. *Transition Met.* **2008**, *33*, 967.
(23) Hudák, J.; Boča, R.; Dlháň, L.; Kožíšek, J.; Moncol, J. *Polyhedron* **2011**, *30*, 1367.
(24) Lin, J.-L.; Fei, S.-T.; Lei, K.-W.; Zheng, Y.-Q. *Acta Crystallogr.* **2006**, *E62*, m2439.
(25) Zhang, X. L.; Ng, S. W. *Acta Crystallogr.* **2005**, *E61*, m1140.
(26) Atanasov, M.; Comba, P. J. *Mol. Struct.* **2007**, *838*, 157.
(27) Papánková, B.; Boča, R.; Dlháň, L.; Nemec, I.; Titiš, J.; Svoboda, I.; Fuess, H. *Inorg. Chim. Acta* **2010**, *363*, 147.
(28) Griffith, J. S. *The Theory of Transition Metal Ions*; University Press: Cambridge, U.K, 1964.
(29) (a) Figgis, B. N. *Trans. Faraday Soc.* **1961**, *57*, 198. (b) Figgis, B. N. *J. Chem. Soc* **1966**, *A*, 1411. (c) Figgis, B. N. *J. Chem. Soc.* **1967**, *A*, 442.
(30) Šebová, M.; Boča, R.; Dlháň, L.; Nemec, I.; Papánková, B.; Pavlik, J.; Fuess, H. *Inorg. Chim. Acta* **2011**, *30*, 1163.